JCTC Journal of Chemical Theory and Computation

Article

pubs.acs.org/JCTC

# Accurate Surface Chemistry beyond the Generalized Gradient Approximation: Illustrations for Graphene Adatoms

Benjamin G. Janesko,*[,†] Veronica Barone,[‡] and Edward N. Brothers[§]

[†]Department of Chemistry, Texas Christian University, Fort Worth, Texas 76129, United States

[‡]Department of Physics, Central Michigan University, Mt. Pleasant, Michigan 48859, United States

[§]Chemistry Department, Texas A&M University at Qatar, Texas A&M Engineering Building, Education City, Doha, Qatar

Supporting Information

**ABSTRACT:** Simulations of surface chemistry often use density functional theory with generalized gradient approximations (GGAs) for the exchange-correlation functional. GGAs have well-known limitations for gas-phase chemistry, including underestimated reaction barriers, and are largely superseded by meta-GGAs and hybrids. Our simulations of O and Li adatoms on graphene add to a growing body of evidence that GGAs have similar limitations on surfaces and that meta-GGAs and screened hybrids are computationally feasible for such systems. Meta-GGAs and screened hybrids systematically improve accuracy, just as they do for gas-phase chemistry, motivating their continued exploration in surface chemistry.

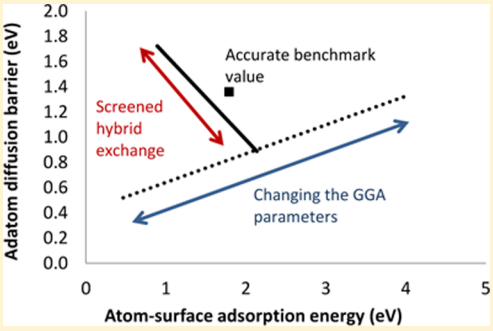


## INTRODUCTION

Adsorption, diffusion, and reactions of molecules on surfaces are central to heterogeneous catalysis and nanomaterials chemistry.[1] Simulations of these processes can provide mechanistic insight and even predictions of new catalysts.[2,3] Such simulations often use Kohn−Sham density functional theory (DFT) for its balance of accuracy and computational expense. This balance is largely governed by the choice of approximation for the many-body exchange-correlation (XC) density functional. DFT simulations of reactions on surfaces typically use generalized gradient approximations (GGAs).[2−6] These model the XC energy density at each point $\mathbf{r}$ as a function of the electron density $\rho(\mathbf{r})$ and its gradient. GGAs are computationally inexpensive and can be tuned to predict adsorption energies. Standard GGAs for surfaces reproduce chemisorption energies within 0.1−0.2 eV.[7,8] Newer dispersion-corrected GGAs[9,10] can give improved accuracy.[11−13] Several recent studies illustrate that GGAs remain the primary tool of computational heterogeneous catalysis.[2−6]

Unfortunately, GGAs systematically overdelocalize electrons.[14] This is problematic for gas-phase chemistry, yielding a range of errors, including overstabilization of the stretched bonds of transition states and underestimation of reaction barriers.[15,16] In contrast to gas-phase chemistry,[17] there are relatively few accurate benchmark values for the height of individual reaction barriers on surfaces. However, existing accurate ab initio calculations indicate that these errors carry over to surfaces: GGAs tuned to predict chemisorption energies systematically underestimate reaction barriers.[18−25] (We have reviewed this literature in our study of ammonia on silicon.[26]) Experimental rates may be reproduced by error cancellation, for example, between too-small adsorption energies and underestimated reaction barriers of adsorbed species.[12] To illustrate, a recent study of ammonia synthesis over ruthenium found that two different GGAs both reproduced the experimental turnover frequency to within an order of magnitude, despite a 0.6 eV discrepancy in the predicted rate-limiting barrier.[2] While such error cancellations are acceptable for many applications, improvements are clearly desirable. Efforts to fix this problem with empirical GGAs[11] and "specific reaction parameter" GGAs fit to individual reactions[27,28] have remaining limitations.[29]

For molecules, a very successful strategy[16] for fixing GGAs' overdelocalization is to incorporate the noninteracting kinetic energy density (meta-GGAs)[30−32] or nonlocal exact exchange (hybrids).[14,33] To illustrate, the carefully designed dispersion-corrected 30-parameter BEEF-vdW GGA gives mean absolute deviations for representative gas-phase heats of formation[34] and reaction barriers[17] of 0.19 and 0.26 eV. (The latter corresponds to an ∼4 order of magnitude error in room-temperature Arrhenius rates.) The 3-parameter hybrid B3LYP[35,36] gives errors of 0.21 and 0.17 eV.[11] Screened hybrids omitting expensive long-range nonlocal exchange[37−39] and accurate empirical meta-GGAs[31,32] have made these approximations practical for solids and surfaces and have been implemented in standard electronic structure codes.[40,41] Encouraging initial results include demonstrations that the HSE06 screened hybrid[37,42] and the M06L[31] and revTPSS[43] meta-GGAs provide improved (though not always perfect) treatments[44−46] for the adsorption site of CO on transition-metal (111) surfaces.[47] However, these methods have so far seen limited application to reactions on surfaces.[26,43,44,46,48,49]

**Received:** August 19, 2013
**Published:** October 21, 2013

   dx.doi.org/10.1021/ct400736w | J. Chem. Theory Comput. 2013, 9, 4853−4859

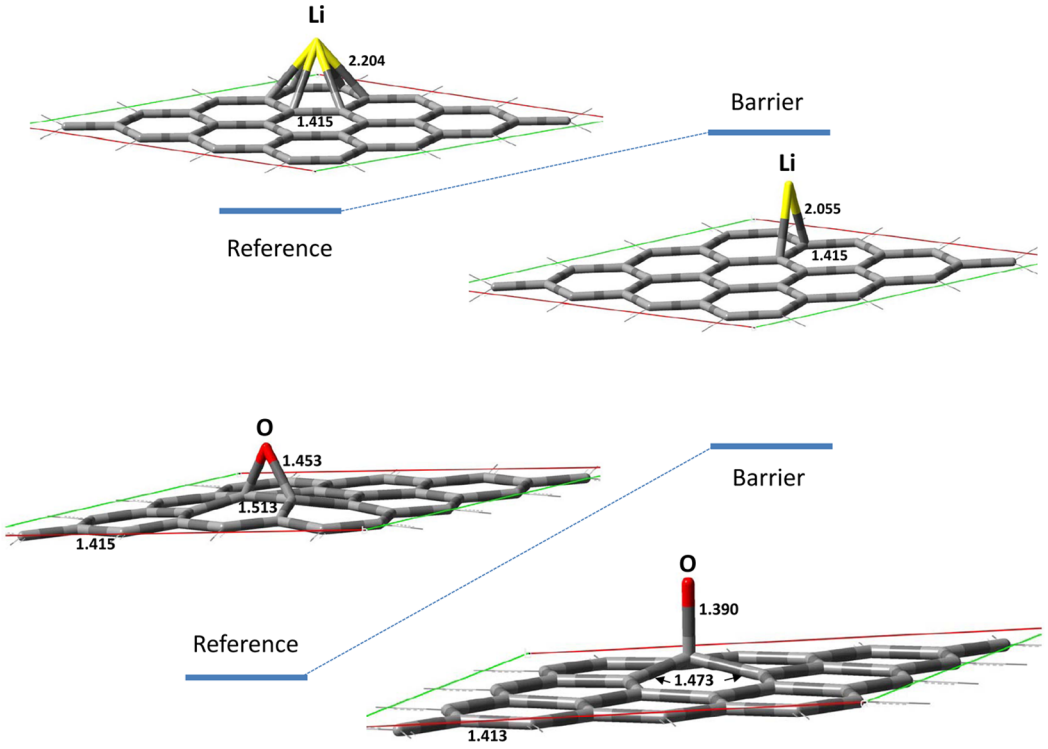


**Figure 1.** Scheme of the unit cell used to calculate the energetics of Li and O adsorbed on graphene.

Adatoms on graphitic nanostructures have been extensively studied for applications such as Li-ion batteries and hydrogen storage media.[50−52] DFT with the local density approximation (LDA) predicts Li diffusion coefficients on graphene that are near the low end of the broad experimental range.[53,54] While GGAs predict faster diffusion,[55] adatoms on graphene exemplify GGAs' general limitations for surface chemistry. A recent ab initio quantum Monte Carlo study showed that standard GGAs severely underestimate diffusion barriers for O adatoms adsorbed on graphene.[24]

Here, we show that meta-GGAs and screened hybrids systematically increase predicted diffusion barriers for O and Li adsorbed on graphene, and better match available ab initio benchmarks. These improvements are largely orthogonal to the effects of dispersion corrections.[12] Screened exchange admixture to a GGA enables simultaneous optimization of both adsorption energies and diffusion barriers, just as it enables simultaneous optimization of both gas-phase thermochemistry and kinetics.[16] As in previous studies, results from these specific cases are arguably generalizable to a broad range of surface science systems.[12,16,56] These results, combined with our report that these functionals improve $NH_3$ dissociation barriers on surfaces[26] and other reports of their successful application to surface chemistry,[43,45,46,48,49] suggest that meta-GGAs and screened hybrids should be vigorously explored in modeling diffusion and reactions on surfaces.

## METHODOLOGY

We report representative XC functionals' predictions for low-coverage O and Li adsorption and diffusion on the hexagonal (h), bridge (b), and top (t) sites of graphene. $\Delta E_x^{ads}$ and $\Delta E_{x\rightarrow y}$ denote adsorption energy to site $x$ and diffusion barrier over site $y$. As in ref 57, we assume that diffusion barriers are equal to the differences between adsorption energies at different sites. For example, $\Delta E_{b\rightarrow t}$ assumes that diffusion of O atoms between adjacent bridge sites occurs along a path through the top site and that the difference between adsorption energies at the bridge and atop sites equals the diffusion barrier. (Higher diffusion barriers over other sites are explored in the Supporting Information.)

Calculations focus on trends among GGAs with different enhancement factors. GGAs model the XC energy density at point $\mathbf{r}$ as the LDA value, which is numerically exact for homogeneous systems, times enhancement factors depending on $|\nabla\rho(\mathbf{r})|$. We test the LDA[58] and (in approximate order of increasing enhancement factor) the PBEsol,[59] PBE,[60] PW91,[61] BPW91,[61,62] RPBE,[7] and BLYP[63] GGAs. We compare these to the nonempirical Tao−Perdew−Staroverov−Scuseria (TPSS) meta-GGA;[30] the empirical M06-L meta-GGA;[31] the HSE06[37,42,64] and HISS[65] screened hybrids; the PBE0,[66,67] B3PW91, and B3LYP global hybrids;[35,36,68] and internuclear dispersion corrections.[9]

Our calculations use the development version of the Gaussian suite of programs.[69] Calculations on graphene sheets use the atom-centered 6-31G** basis set and periodicity in two dimensions. Calculations for Li on graphene use a repeating unit with 64 C and 2 Li atoms per cell, giving a spin multiplicity of 1. Periodic calculations use 200 $k$ points and evaluate the screened exchange and nonlocal one-electron operators using at least 135 replica cells.[70] Test calculations (not shown) suggest that global hybrid calculations require a very large number of replica cells for complete convergence. Global hybrids are reported here solely to confirm the qualitative trends seen with screened hybrids. Coulomb terms are evaluated using infinite lattice sums via the fast multipole moment algorithm.[71] Basis set superposition errors are ignored throughout.

All calculations use SVWN/6-31G** geometries to enable "apples-to-apples" comparison of different functionals' energetic effects. (SVWN denotes Gaspár−Kohn−Sham local density approximation exchange and Vosko−Wilk−Nusair

correlation functional III.[58]) Geometries for Li on graphene are taken from ref 57, and geometries for O on graphene are optimized following ref 57, as shown in Figure 1. Test SVWN/6-31G** calculations reproduce energy barriers of ref 57 to within 0.001 eV. Geometries for Li on naphthalene use the SVWN/6-31G** geometry of isolated naphthalene, with Li constrained to hexagonal or bridge sites. Calculations in Figures 2, 3, and 4 are performed post-PBE; select self-consistent calculations are reported in the Supporting Information.

Benchmark calculations for Li on naphthalene are performed using CCSD(T)/CBS and combine a two-point extrapolation of the Hartree−Fock energy in the cc-pVTZ ("TZ") and cc-pVQZ ("QZ") basis sets using the formulas of Haliker and co-workers,[72] a two-point extrapolation of the MP2 correlation energy in the TZ and QZ basis sets,[73] and a ΔCCSD(T) correction in the TZ basis set. Correlated calculations use the default frozen cores so that the isolated Li atom has one correlated valence electron and zero correlation energy. DFT calculations on these open-shell systems use stability analysis[74] to locate a stable unrestricted Kohn−Sham state. These calculations converge to an ionic structure for the initial Li adsorption,[56,75] as detailed in the Supporting Information.

## RESULTS AND DISCUSSION

Figure 2 plots predicted diffusion barriers vs adsorption energies for adatoms on graphene. The top panel plots O $\Delta E_{b\to t}$ vs $\Delta E_b^{ads}$, the bottom panel Li $\Delta E_{h\to b}$ vs $\Delta E_h^{ads}$. Similar results are seen for diffusion over other sites and for F on graphene (Supporting Information).

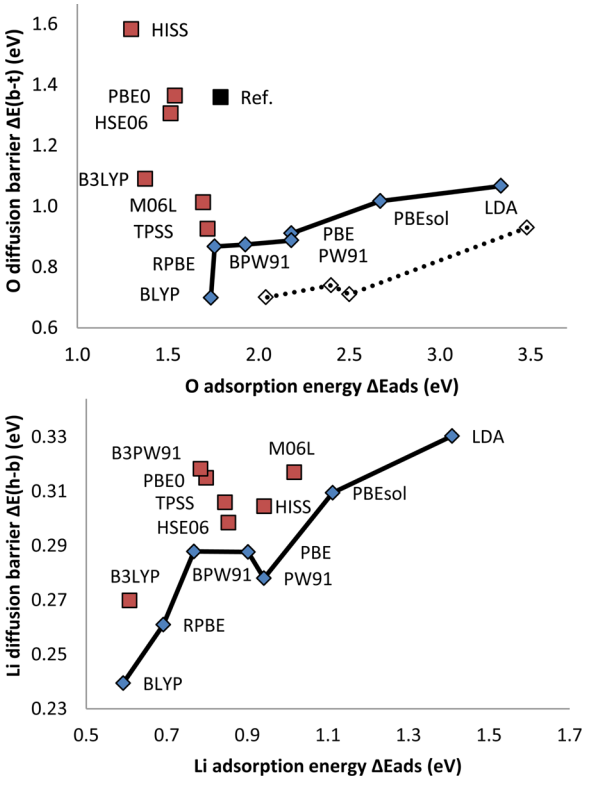


**Figure 2.** Predicted diffusion barriers vs adsorption energies for O (top) and Li (bottom) on graphene. Lines + points are the LDA and GGAs; points are meta-GGAs and screened hybrids. Open symbols (from left to right: revPBE, PW91, PBE, LDA) and "Ref." diffusion Monte Carlo are from ref 24.

The nearly constant shift between our calculations and ref 24 appears to arise from the choice of geometry, basis set superposition error, and other details of the calculation. Test calculations (Supporting Information) illustrate that the absolute O atom diffusion barrier is rather sensitive to calculation details, the Li diffusion barrier is less sensitive, and the trends in Figure 2 are robust to changes in the computational details.

For both O and Li, GGAs give a nearly linear relation between calculated adsorption barriers and reaction energies. (Note the different scales: PBE and PW91 agree to within 0.02 eV for O $\Delta E_{b\to t}$, and to within 0.01 eV for Li $\Delta E_{h\to b}$.) GGA correlation has a modest influence, with the BPW91 (BLYP) GGA predicting relatively high (low) diffusion barriers for Li (O). Most importantly, no calculation along this trend approaches the benchmark for O diffusion, despite the wide range in predicted adsorption energies. Other empirical GGAs[76] do not improve matters (Supporting Information). In contrast, all meta-GGAs and screened hybrids give diffusion barriers above the GGA trend. The effect is modest for Li and large for O, where the results are much closer to the benchmark. This extends previous evidence for GGAs' underestimation of barriers on surfaces.[18−26]

Figure 3 confirms these results using ab initio benchmarks (complete-basis-set-extrapolated coupled cluster) for Li on a

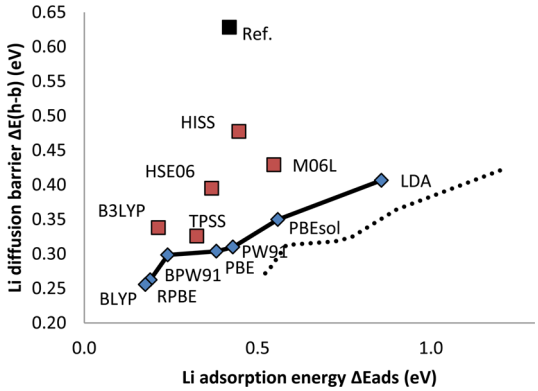


**Figure 3.** Predicted diffusion barrier vs adsorption energy for Li on a graphene cluster model, including CCSD(T) benchmarks "Ref". Dotted line denotes dispersion-corrected GGAs.

finite cluster model of graphene. While this small cluster is emphatically not a perfect representation of a graphene surface, it recovers the important trends from Figure 2. Meta-GGAs, screened hybrids, and global hybrids substantially increase the diffusion barriers. They also match the benchmark better than any GGA. Unscaled "−D" dispersion corrections[9] increase the GGAs' adsorption energies but do not significantly affect diffusion barriers. This reiterates that GGA overdelocalization is largely orthogonal to dispersion effects. (Dispersion corrections are likely not necessary for adsorption of O and Li on graphene and are included solely to illustrate that dispersion does not fix GGA diffusion barriers.)

Figure 2 suggests that, just as for gas-phase chemistry,[31,33,35] efforts to design functionals that accurately treat both thermodynamics and kinetics on surfaces benefit from going beyond the GGA. Figure 4 reiterates this, showing how systematic variations in a functional's GGA enhancement and screened exchange admixture affect its predictions for gas-phase


dx.doi.org/10.1021/ct400736w | J. Chem. Theory Comput. 2013, 9, 4853−4859

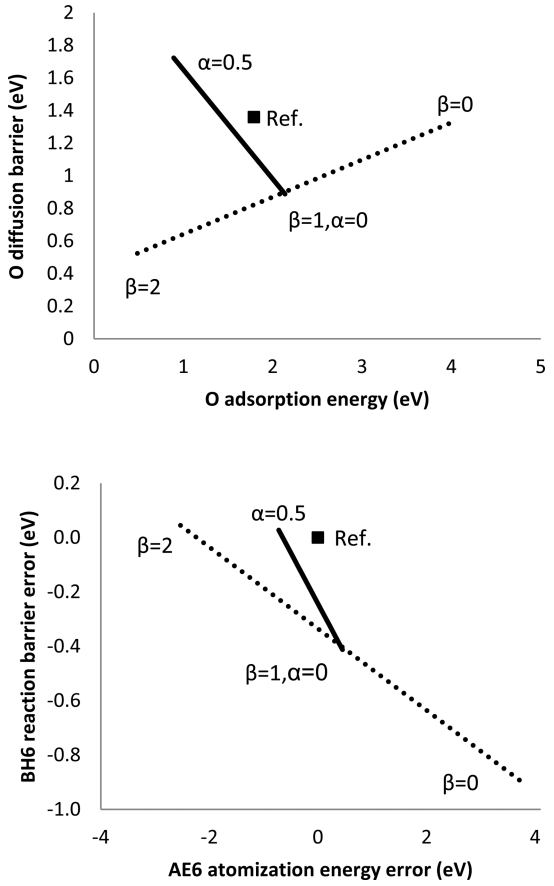


**Figure 4.** Systematic variations in a GGA's enhancement factor $\beta$ (dotted lines) and screened exact exchange admixture $\alpha$ (solid lines), from eq 1. (Top) Barrier vs adsorption energy for O on graphene. (Bottom) Mean signed errors in gas-phase kinetics vs thermochemistry. "Ref." are diffusion Monte Carlo from ref 24 (top) and zero mean signed error (bottom).

and surface chemistry. We combine PBE correlation with the tunable exchange functional

$$E_X = E_X^{LDA} + \alpha(E_X^{SR-Ex} - E_X^{SR-PBE}) + \beta(E_X^{PBE} - E_X^{LDA}) \quad (1)$$

$\alpha$ controls the admixture of screened exact exchange $E_X^{SR-Ex}$. $\beta$ controls the GGA enhancement factor. (Note that "specific reaction parameter" functionals originally tuned a global hybrid's $\alpha$ and $\beta$.[27]) Screened exchange uses the HSE06 $\omega$ = 0.11 bohr$^{-1}$.[42] The top panel of Figure 4 shows $\Delta E_{b\to t}$ vs $\Delta E_b^{ads}$ for O on graphene as in Figure 2. The bottom panel shows mean signed errors in the small, representative AE6 set of atomization energies and BH6 set of gas-phase reaction barriers.[77] Dotted lines show variations in $\beta$ at $\alpha$ = 0; solid lines show variations in $\alpha$ at $\beta$ = 1. The two lines do not quite match at $\beta$ = 1,$\alpha$ = 0 due to residual differences between full- and short-range PBE exchange. Li on graphene gives similar trends (Supporting Information).

Figure 4 confirms the utility of the screened exchange admixture. Turning off the GGA exchange enhancement $\beta$ = 0 gives large $\Delta E_b^{ads}$ and large $\Delta E_{b\to t}$ like the LDA. Increasing the GGA enhancement $\beta$ decreases $\Delta E_b^{ads}$ and $\Delta E_{b\to v}$, as in Figures 2 and 3. In contrast, increasing the screened exchange admixture $\alpha$ increases both gas-phase and surface reaction barriers with modest variations in adsorption energies and thermochemistry. We conclude that, just as for gas-phase chemistry,[35,36] simultaneous variation of the GGA form and the nonlocal exchange admixture allows optimization of both thermodynamics and kinetics on surfaces.

## CONCLUSIONS

Our calculations for adatoms on graphene illustrate the broad result that the DFT XC functional is critical for determining predicted adsorption energies and diffusion barriers on surfaces. Comparisons with accurate benchmarks are consistent with previous demonstrations[18−26] that even dispersion-corrected GGAs can underestimate diffusion and reaction barriers on surfaces, just as they underestimate gas-phase barriers. Figure 4 shows that the screened exchange admixture can improve reaction barriers on surfaces and reiterates its familiar improvements to gas-phase kinetics. Indeed, from one perspective, Figure 4 carries the discouraging implication that empirical tuning will give any number that one wants! Our perspective is somewhat more hopeful. Computational chemists have long combined modification of the GGA form,[78] incorporation of the kinetic energy density,[30] exact exchange admixture,[36] and dispersion corrections[10] to construct modestly empirical, physically motivated XC functionals that capture a broad range of phenomena for small- and medium-sized molecules. One need only consider the widespread use of Becke's three-parameter global hybrids[35,36] and their successors[79−81] to see the success of this strategy. We suggest that this strategy is even more valuable for surfaces due to the challenges of ab initio calculations on these systems. We conclude that the combination of modified GGA forms, incorporation of the kinetic energy density and/or screened exact exchange, dispersion corrections, and a few empirical parameters that has demonstrated such success in gas-phase chemistry could significantly aid current efforts in improving simulations of reaction kinetics and thermodynamics on surfaces. These limitations of GGAs also motivate continued development of nonempirical ab initio methods for surface chemistry.[82] However, we suggest that modestly empirical DFT methods will continue to provide a valuable option for systems beyond the reach of ab initio calculations.

## ASSOCIATED CONTENT

### Supporting Information

The Supporting Information includes all calculated geometries and total energies, as well as test calculations with different basis sets. This material is available free of charge via the Internet at http://pubs.acs.org.

## AUTHOR INFORMATION

### Corresponding Author

*E-mail: b.janesko@tcu.edu.

### Notes

The authors declare no competing financial interest.

## ACKNOWLEDGMENTS

B.G.J. and E.N.B. acknowledge support from the Qatar National Research Foundation through the National Priorities Research Program (NPRP Grant No. 09-143-1-022). V.B. acknowledges support from NSF CBET-1335944.

## REFERENCES


(1) Peet, J.; Heeger, A. J.; Bazan, G. C. "Plastic" Solar Cells: Self-Assembly of Bulk Heterojunction Nanomaterials by Spontaneous Phase Separation. *Acc. Chem. Res.* **2009**, *42*, 1700.

(2) Honkala, K.; Hellman, A.; Remediakis, I. N.; Logadottir, A.; Carlsson, A.; Dahl, S.; Christiansen, C. H.; Nørskov, J. K. Ammonia Synthesis from First-Principles Calculations. *Science* **2005**, *307*, 555.

(3) Nørskov, J. K.; Abild-Pedersen, F.; Studt, F.; Bligaard, T. Density Functional Theory in Surface Chemistry and Catalysis. *Proc. Natl. Acad. Sci. U.S.A.* **2011**, *108*, 937.

(4) Chia, M.; Pagán-Torres, Y. J.; Hibbitts, D.; Tan, Q.; Pham, H. N.; Datye, A. K.; Neurock, M.; Davis, R. J.; Dumesic, J. A. Selective Hydrogenolysis of Polyols and Cyclic Ethers over Bifunctional Surface Sites on Rhodium−Rhenium Catalysts. *J. Am. Chem. Soc.* **2011**, *133*, 12675−12689.

(5) Kou, R.; Shao, Y.; Mei, D.; Nie, Z.; Wang, D.; Wang, C.; Viswanathan, V. V.; Park, S.; Aksay, I. A.; Lin, Y.; et al. Stabilization of Electrocatalytic Metal Nanoparticles at Metal−Metal Oxide−Graphene Triple Junction Points. *J. Am. Chem. Soc.* **2011**, *133*, 2541−2547.

(6) Jung, J.; Shin, H.-J.; Kim, Y.; Kawai, M. Ligand Field Effect at Oxide−Metal Interface on the Chemical Reactivity of Ultrathin Oxide Film Surface. *J. Am. Chem. Soc.* **2012**, *134*, 10554−10561.

(7) Hammer, B.; Hansen, L. B.; Nørskov, J. K. Improved Adsorption Energetics within Density-Functional Theory Using Revised Perdew-Burke-Ernzerhof Functionals. *Phys. Rev. B* **1999**, *59*, 7413.

(8) Zhang, Y.; Yang, W. Comment on "Generalized Gradient Approximation Made Simple. *Phys. Rev. Lett.* **1998**, *80*, 890.

(9) Antony, J.; Grimme, S. Density Functional Theory Including Dispersion Interactions for Intermolecular Interactions in a Large Benchmark Set of Biologically Relevant Molecules. *Phys. Chem. Chem. Phys.* **2006**, *8*, 5287.

(10) Johnson, E. R.; Mackie, I. D.; DiLabio, G. A. Dispersion Interactions in Density-Functional Theory. *J. Phys. Org. Chem.* **2009**, *22*, 1127.

(11) Wellendorff, J.; Lundgaard, K. T.; Møgelhøj, A.; Petzold, V.; Landis, D. D.; Nørskov, J. K.; Bligaard, T.; Jacobsen, K. W. Density Functionals for Surface Science: Exchange-Correlation Model Development with Bayseian Error Estimation. *Phys. Rev. B* **2012**, *85*, 235149.

(12) Gomes, J.; Zimmerman, P. M.; Head-Gordon, M.; Bell, A. T. Accurate Prediction of Hydrocarbon Interactions with Zeolites Utilizing Improved Exchange-Correlation Functionals and QM/MM Methods: Benchmark Calculations of Adsorption Enthalpies and Application to Ethylene Methylation by Methanol. *J. Phys. Chem. C* **2012**, *116*, 15406−15414.

(13) Studt, F. T.; Abild-Pedersen, F.; Varley, J. B.; Nø rskov, J. K. CO and $CO_2$ Hydrogenation to Methanol Calculated Using the BEEF-vdW Functional. *Catal. Lett.* **2013**, *143*, 71−73.

(14) Csonka, G. I.; Perdew, J. P.; Ruzsinszky, A. Global Hybrid Functionals: A Look at the Engine under the Hood. *J. Chem. Theory Comput.* **2010**, *6*, 3688−3703.

(15) Madriossian, N.; Parkhill, J. A.; Head-Gordon, M. Benchmark Results for Empirical Post-GGA Functionals: Difficult Exchange Problems and Independent Tests. *Phys. Chem. Chem. Phys.* **2011**, *13*, 19325−19337.

(16) Yang, K.; Zheng, J.; Zhao, Y.; Truhlar, D. G. Tests of the RPBE, revPBE, $\tau$-HCTHhyb, $\omega$B97X-D, and MOHLYP Density Functional Approximations and 29 Others against Representative Databases for Diverse Bond Energies and Barrier Heights in Catalysis. *J. Chem. Phys.* **2010**, *132*, 164117.

(17) Zheng, J.; Zhao, Y.; Truhlar, D. G. The DBH24/08 Database and Its Use To Assess Electronic Structure Model Chemistries for Chemical Reaction Barrier Heights. *J. Chem. Theory Comput.* **2009**, *5*, 808.

(18) Filippi, C.; Healy, S. B.; Kratzer, P.; Pehlke, E.; Scheffler, M. Quantum Monte Carlo Calculations of $H_2$ Dissociation on Si(001). *Phys. Rev. Lett.* **2002**, *89*, 166102.

(19) Dürr, M.; Raschke, M. B.; Pehlke, E.; Höfer, U. Structure Sensitive Reaction Channels of Molecular Hydrogen on Silicon Surfaces. *Phys. Rev. Lett.* **2001**, *86*, 123−126.

(20) Nachtigall, P.; Jordan, K. D.; Smith, A.; Jónsson, H. Investigation of the Reliability of Density Functional Methods: Reaction and Activation Energies for Si−Si Bond Cleavage and $H_2$ Elimination from Silanes. *J. Chem. Phys.* **1996**, *104*, 148.

(21) Pozzo, M.; Alfè, D. Hydrogen Dissociation on Mg(0001) Studied via Quantum Monte Carlo Calculations. *Phys. Rev. B* **2008**, *78*, 245313.

(22) Kanai, Y.; Takeuchi, N. Towards Accurate Reaction Energetics for Molecular Line Growth at Surface: Quantum Monte Carlo and Density Functional Theory Calculations. *J. Chem. Phys.* **2009**, *131*, 214708.

(23) de Jong, G. T.; Bickelhaupt, F. M. Oxidative Addition of the Fluoromethane C−F bond to Pd. An ab Initio Benchmark and DFT Validation Study. *J. Phys. Chem. A* **2005**, *109*, 9685.

(24) Hsing, C. R.; Wei, C. M.; Chou, M. Y. Quantum Monte Carlo Investigations of Adsorption Energetics on Graphene. *J. Phys.: Condens. Matter* **2012**, *24*, 395002.

(25) Hoggan, P. E. Quantum Monte Carlo Simulation of Carbon Monoxide Reactivity When Adsorbed at Metal and Oxide Catalyst Surfaces: Trial Wave-Functions with Exponential Type Basis and Quasi-Exact Three-Body Correlation. *Int. J. Quantum Chem.* **2013**, *113*, 277−285.

(26) Sniatynsky, R.; Janesko, B. G.; El-Mellouhi, F.; Brothers, E. N. Application of Screened Hybrid Density Functional Theory to Ammonia Decomposition on Silicon. *J. Phys. Chem. C* **2012**, *116*, 26396−26404.

(27) Chuang, Y.-Y.; Radhakrishnan, M. L.; Fast, P. L.; Cramer, C. J.; Truhlar, D. G. Direct Dynamics for Free Radical Kinetics in Solution: Solvent Effect on the Rate Constant for the Reaction of Methanol with Atomic Hydrogen. *J. Phys. Chem. A* **1999**, *103*, 4893−4909.

(28) Díaz, C.; Pijper, E.; Olsen, R. A.; Busnengo, H. F.; Auerbach, D. J.; Kroes, G. J. Chemically Accurate Simulation of a Prototypical Surface Reaction: $H_2$ Dissociation on Cu(111). *Science* **2009**, *326*, 832−834.

(29) Kroes, G.-J. Towards Chemically Accurate Simulation of Molecule−Surface Reactions. *Phys. Chem. Chem. Phys.* **2012**, *14*, 14966−14981.

(30) Tao, J.; Perdew, J. P.; Staroverov, V. N.; Scuseria, G. E. Climbing the Density Functional Ladder: Nonempirical Meta-Generalized Gradient Approximation Designed for Molecules and Solids. *Phys. Rev. Lett.* **2003**, *91*, 146401.

(31) Zhao, Y.; Truhlar, D. G. A New Local Density Functional for Main-Group Thermochemistry, Transition Metal Bonding, Thermochemical Kinetics, and Noncovalent Interactions. *J. Chem. Phys.* **2006**, *125*, 194101.

(32) Peverati, R.; Truhlar, D. G. M11-L: A Local Density Functional That Provides Improved Accuracy for Electronic Structure Calculations in Chemistry and Physics. *J. Phys. Chem. Lett.* **2012**, *3*, 117.

(33) Becke, A. D. A New Mixing of Hartee−Fock and Local Density-Functional theories. *J. Chem. Phys.* **1993**, *98*, 1372.

(34) Curtiss, L. A.; Raghavachari, K.; Redfern, P. C.; Pople, J. A. Assessment of Gaussian-3 and Density Functional Theories for a Larger Experimental Test Set. *J. Chem. Phys.* **2000**, *112*, 7374−7382.

(35) Becke, A. D. Density-Functional Thermochemistry. III. The Role of Exact Exchange. *J. Chem. Phys.* **1993**, *98*, 5648−5652.

(36) Stephens, P. J.; Devlin, F. J.; Chabalowski, C. F.; Frisch, M. J. Ab Initio Calculation of Vibrational Absorption and Circular Dichroism Spectra Using Density Functional Force Fields. *J. Phys. Chem.* **1994**, *98*, 11623−11627.

(37) (a) Heyd, J.; Scuseria, G. E.; Ernzerhof, M. Hybrid Functionals Based on a Screened Coulomb Potential. *J. Chem. Phys.* **2003**, *118*, 8207−8215;(b) **2006**, *124*, 219906.

(38) Marsman, M.; Paier, J.; Stroppa, A.; Kresse, G. Hybrid Functionals Applied to Extended Systems. *J. Phys.: Condens. Matter* **2008**, *20*, 064201.

(39) Stroppa, A.; Kresse, G. The Shortcomings of Semi-local and Hybrid Functionals: What We Can Learn from Surface Science Studies. *New J. Phys.* **2008**, *10*, 063020.
(40) Zhao, Y.; Truhlar, D. A. Exploring the Limit of Accuracy of the Global Hybrid Meta Density Functional for Main-Group Thermochemistry, Kinetics, and Noncovalent Interactions. *J. Chem. Theory Comput.* **2008**, *4*, 1849−1868.
(41) Janesko, B. G.; Henderson, T. M.; Scuseria, G. E. Screened Hybrid Density Functionals for Solid-State Chemistry and Physics. *Phys. Chem. Chem. Phys.* **2009**, *11*, 443−454.
(42) Krukau, A. V.; Vydrov, O. A.; Izmaylov, A. F.; Scuseria, G. E. Influence of the Exchange Screening Parameter on the Performance of Screened Hybrid Functionals. *J. Chem. Phys.* **2006**, *125*, 224106.
(43) Perdew, J. P.; Ruzsinszky, A.; Csonka, G. I.; Constantin, L. A.; Sun, J.-W. Workhorse Semilocal Density Functional for Condensed Matter Physics and Quantum Chemistry. *Phys. Rev. Lett.* **2009**, *103*, 026403.
(44) Stroppa, A.; Termentzidis, K.; Paier, J.; Kresse, G.; Hafner, J. CO Adsorption on Metal Surfaces: A Hybrid Functional Study with Plane-Wave Basis Set. *Phys. Rev. B* **2007**, *76*, 195440.
(45) Sun, J.; Marsman, M.; Ruzsinszky, A.; Kresse, G.; Perdew, J. P. Improved Lattice Constants, Surface Energies, and CO Desorption Energies from a Semilocal Density Functional. *Phys. Rev. B* **2011**, *83*, 121410.
(46) Luo, S.; Zhao, Y.; Truhlar, D. G. Improved CO Adsorption Energies, Site Preferences, and Surface Formation Energies from a Meta-Generalized Gradient Approximation Exchange-Correlation Functional, M06-L. *J. Phys. Chem. Lett.* **2012**, *3*, 2975−2979.
(47) Feibelman, P. J.; Hammer, B.; Nørskov, J. K.; Wagner, F.; Scheffler, M.; Stumpf, R.; Watwe, R.; Dumesic, J. The CO/Pt(111) Puzzle. *J. Phys. Chem. B* **2001**, *105*, 4018.
(48) Demers-Carpentier, V.; Rasmussen, A. M. H.; Goubert, G.; Ferrighi, L.; Dong, Y.; Lemay, J.-C.; Masini, F.; Zeng, Y.; Hammer, B.; McBreen, P. H. Stereodirection of an $\alpha$-Ketoester at Sub-molecular Sites on Chirally Modified Pt(111): Heterogeneous Asymmetric Catalysis. *J. Am. Chem. Soc.* **2013**, *135*, 9999−10002.
(49) Balog, R.; Andersen, M.; Jørgensen, B.; Sljivancanin, Z.; Hammer, B.; Baraldi, A.; Larciprete, R.; Hofmann, P.; Hornekær, L.; Lizzit, S. Controlling Hydrogenation of Graphene on Ir(111). *ACS Nano* **2013**, *7*, 3823−3832.
(50) Liang, M.; Zhi, L. Graphene-Based Electrode Materials for Rechargable Lithium Batteries. *J. Mater. Chem.* **2009**, *19*, 5871−5878.
(51) Huang, X.; Qi, X.; Boey, F.; Zhang, H. Graphene-Based Composites. *Chem. Soc. Rev.* **2012**, *41*, 666−686.
(52) Bhardwaj, T.; Antic, A.; Pavan, B.; Barone, V.; Fahlman, B. D. Enhanced Electrochemical Lithium Storage by Graphene Nanoribbons. *J. Am. Chem. Soc.* **2010**, *132*, 12556−12558.
(53) Toyoura, K.; Koyama, Y.; Kuwabara, A.; Tanaka, I. Effects of Off-Stoichiometry of $LiC_6$ on the Lithium Diffusion Mechanism and Diffusivity by First Principles Calculations. *J. Phys. Chem. C* **2010**, *114*, 2375.
(54) Mandeltort, L.; Yates, J. T., Jr. Rapid Atomic Li Surface Diffusion and Intercalation on Graphite: A Surface Science Study. *J. Phys. Chem. C* **2012**, *116*, 24962.
(55) Kubota, Y.; Ozawa, N.; Nakanishi, H.; Kasai, H. Quantum States and Diffusion of Lithium Atom Motion on a Graphene. *J. Phys. Soc. Jpn.* **2010**, *79*, 014601.
(56) Baker, T. A.; Head-Gordon, M. Modeling the Charge Transfer between Alkali Metals and Polycyclic Aromatic Hydrocarbons Using Electronic Structure Methods. *J. Phys. Chem. A* **2010**, *114*, 10326.
(57) Uthaisar, C.; Barone, V. Edge Effects on the Characteristics of Li Diffusion in Graphene. *Nano Lett.* **2010**, *10*, 2838.
(58) Vosko, S. H.; Wilk, L.; Nusair, M. Accurate Spin-Dependent Electron Liquid Correlation Energies for Local Spin Density Calculations: A Critical Analysis. *Can. J. Phys.* **1980**, *58*, 1200−1211.
(59) Perdew, J. P.; Ruzsinszky, A.; Csonka, G. A.; Vydrov, O. A.; Scuseria, G. E.; Constantin, L. I.; Zhou, X.; Burke, K. Restoring the Density-Gradient Expansion for Exchange in Solids and Surfaces. *Phys. Rev. Lett.* **2008**, *100*, 136406.
(60) (a) Perdew, J. P.; Burke, K.; Ernzerhof, M. Generalized Gradient Approximation Made Simple. *Phys. Rev. Lett.* **1996**, *77*, 3865−3868; (b) **1997**, *78*, 1396(E).
(61) Perdew, J. P. In *Electronic Structure of Solids '91*; Ziesche, P., Eschrig, H., Eds.; Akademie Verlag: Berlin, 1991.
(62) Becke, A. D. Density-Functional Exchange-Energy Approximation with Correct Asymptotic Behavior. *Phys. Rev. A* **1988**, *38*, 3098.
(63) Lee, C.; Yang, W.; Parr, R. G. Development of the Colle-Salvetti Correlation-Energy Formula into a Functional of the Electron Density. *Phys. Rev. B* **1988**, *37*, 785.
(64) Henderson, T. M.; Janesko, B. G.; Scuseria, G. E. Generalized Gradient Approximation Model Exchange Holes for Range-Separated Hybrids. *J. Chem. Phys.* **2008**, *128*, 194105.
(65) Henderson, T. M.; Izmaylov, A. F.; Scuseria, G. E.; Savin, A. The Importance of Middle-Range Hartree-Fock-type Exchange for Hybrid Density Functionals. *J. Chem. Phys.* **2007**, *127*, 221103.
(66) Adamo, C.; Barone, V. Toward Reliable Density Functional Methods without Adjustable Parameters: The PBE0 Model. *J. Chem. Phys.* **1999**, *110*, 6158−6170.
(67) Ernzerhof, M.; Scuseria, G. E. Assessment of the Perdew−Burke−Ernzerhof Exchange-Correlation Functional. *J. Chem. Phys.* **1999**, *110*, 5029−5036.
(68) Paier, J.; Marsman, M.; Kresse, G. Why Does the B3LYP Hybrid Functional Fail for Metals? *J. Chem. Phys.* **2007**, *127*, 024103.
(69) Frisch, M. J.; Trucks, G. W.; Schlegel, H. B.; Scuseria, G. E.; Robb, M. A.; Cheeseman, J. R.; Scalmani, G.; Barone, V.; Mennucci, B.; Petersson, G. A.; Nakatsuji, H.; Caricato, M.; Li, X.; Hratchian, H. P.; Izmaylov, A. F.; Bloino, J.; Zheng, G.; Sonnenberg, J. L.; Liang, W.; Hada, M.; Ehara, M.; Toyota, K.; Fukuda, R.; Hasegawa, J.; Ishida, M.; Nakajima, T.; Honda, Y.; Kitao, O.; Nakai, H.; Vreven, T.; Montgomery, J. A., Jr.; Peralta, J. E.; Ogliaro, F.; Bearpark, M.; Heyd, J. J.; Brothers, E.; Kudin, K. N.; Staroverov, V. N.; Keith, T.; Kobayashi, R.; Normand, J.; Raghavachari, K.; Rendell, A.; Burant, J. C.; Iyengar, S. S.; Tomasi, J.; Cossi, M.; Rega, N.; Millam, J. M.; Klene, M.; Knox, J. E.; Cross, J. B.; Bakken, V.; Adamo, C.; Jaramillo, J.; Gomperts, R.; Stratmann, R. E.; Yazyev, O.; Austin, A. J.; Cammi, R.; Pomelli, C.; Ochterski, J. W.; Martin, R. L.; Morokuma, K.; Zakrzewski, V. G.; Voth, G. A.; Salvador, P.; Dannenberg, J. J.; Dapprich, S.; Parandekar, P. V.; Mayhall, N. J.; Daniels, A. D.; Farkas, O.; Foresman, J. B.; Ortiz, J. V.; Cioslowski, J.; Fox, D. J. *Gaussian Development Version*, Revision H.31; Gaussian, Inc.: Wallingford, CT, 2010.
(70) Kudin, K. N.; Scuseria, G. E. Linear-Scaling Density-Functional Theory with Gaussian Orbitals and Periodic Boundary Conditions: Efficient Evaluation of Energies and Forces via the Fast Multipole Method. *Phys. Rev. B* **2000**, *61*, 16440−16453.
(71) Kudin, K. N.; Scuseria, G. E. A Fast Multipole Algorithm for the Efficient Treatment of the Coulomb Problem in Electronic Structure Calculations of Periodic Systems with Gaussian Orbitals. *Chem. Phys. Lett.* **1998**, *289*, 611.
(72) Halkier, A.; Helgaker, T.; Jørgensen, P.; Klopper, W.; Olsen, J. Basis-Set Convergence of the Energy in Molecular Hartree−Fock Calculations. *Chem. Phys. Lett.* **1999**, *302*, 437.
(73) Halkier, A.; Helgaker, T.; Jørgensen, P.; Klopper, W.; Koch, H.; Olsen, J.; Wilson, A. K. Basis-Set Convergence in Correlated Calculations on Ne, $N_2$, and $H_2O$. *Chem. Phys. Lett.* **1998**, *286*, 243.
(74) Seeger, R.; Pople, J. A. Self-Consistent Molecular Orbital Methods. XVIII. Constraints and Stability in Hartree−Fock Theory. *J. Chem. Phys.* **1977**, *66*, 3045.
(75) Denis, P. A.; Iribane, F. $C_{2v}$ or $C_{6v}$: Which is the Most Stable Structure of the Benzene-Lithium Complex? *Chem. Phys. Lett.* **2013**, *573*, 15−18.
(76) Boese, A. D.; Doltsinis, N. L.; Handy, N. C.; Sprik, M. New Generalized Gradient Approximation Functionals. *J. Chem. Phys.* **2000**, *112*, 1670.
(77) (a) Lynch, B. J.; Truhlar, D. G. Small Representative Benchmarks for Thermochemical Calculations. *J. Phys. Chem. A* **2003**, *107*, 8996;(b) **2004**, *108*, 1460(E).

(78) Becke, A. D. Density-Functional Thermochemistry. V. Systematic Optimization of Exchange-Correlation Functionals. *J. Chem. Phys.* **1997**, *107*, 8554.
(79) Yanai, T.; Tew, D. P.; Handy, N. C. A New Hybrid Exchange-Correlation Functional Using the Coulomb-Attenuating Method (CAM-B3LYP). *Chem. Phys. Lett.* **2004**, *393*, 51.
(80) Civarelli, B.; Zicovich-Wilson, C. M.; Valenzaon, L.; Ugliengo, P. B3LYP Augmented with an Empirical Dispersion Term (B3LYP-D*) As Applied to Molecular Crystals. *CrystEngComm* **2008**, *10*, 405−410.
(81) Civarelli, B.; Maschio, L.; Ugliengo, P.; Zicovich-Wilson, C. M. Role of Dispersive Interactions in the CO Adsorption on MgO(001): Periodic B3LYP Calculations Augmented with an Empirical Dispersion Term. *Phys. Chem. Chem. Phys.* **2010**, *12*, 6382−6386.
(82) Ren, X.; Rinke, P.; Joas, C.; Scheffler, M. Random-Phase Approximation and Its Applications in Computational Chemistry and Materials Science. *J. Mater. Sci.* **2012**, *47*, 7447−7471.